

# A Low-Cost Inverter for Domestic Fuel Cell Applications

A. M. Tuckey

Powercorp Pty. Ltd.  
Darwin, N.T. Australia  
tuckey@ieee.org

J. N. Krase

University of Wisconsin—Madison  
Madison, WI U.S.A.

**Abstract**—The utilization of fuel cells for distributed power generation requires the development of an inexpensive inverter that converts a fuel cell's variable dc output into useful ac. To encourage this development the US Department of Energy and the IEEE setup and sponsored a national US student competition with a substantial first prize going to the lowest cost working fuel cell inverter: the 2001 Future Energy Challenge (FEC). This paper describes the work of the University of Wisconsin FEC Team. It discusses the topology used to achieve the said objective, the rationale used in choosing this topology, detailed component selection optimized to minimize cost, and the dc/dc and dc/ac converter control. Finally some conclusions are made and a new total-system-approach design using a high voltage fuel cell is proposed to further reduce the cost of the inverter.

**Keywords**—Fuel cell, Renewable Energy, Distributed Generation.

## I. INTRODUCTION

“IN the future, many local energy sources, such as photovoltaic units, fuel cells, small turbines, small hydroelectric plants, and other dispersed sources will become a larger fraction of our electrical supply.” This quote is taken from the 2001 Future Energy Challenge [1], a national US student competition sponsored and set up by the Department of Energy and the IEEE, which spanned Fall 2000 through Summer 2001.

## II. THE 2001 FUTURE ENERGY CHALLENGE

The Challenge sought to “. . . dramatically improve the design and reduce the cost of dc-ac inverters and interface systems for use in distributed generation systems . . . with the goal of making these interface systems practical and cost effective. The objectives are to design elegant, manufacturable systems that would reduce the costs of commercial interface systems by at least 50% to below \$50 per kilowatt and, thereby, accelerate the deployment of distributed generation systems in homes and buildings.”

Fourteen US universities participated in the competition, one being the University of Wisconsin—Madison & Platteville campuses. The UW FEC Team's motto of “*Delivering the Biggest Bang for the Buck!*” was adopted by the 22 undergraduate and graduate students. Participating students' disciplines included Electrical Engineering, Mechanical Engineering, Computer Engineering, Computer Science, Materials Science and Engineering, Engineering Mechanics and Astronautics, and Journalism, and all levels from freshman to PhD were represented.

This paper describes the inverter designed and built by the UW FEC Team. No new technology was used in the

This work was supported by the Wisconsin Electric Machines and Power Electronics Consortium (WEMPEC), American Power Conversion, International Fuel Cells, Motorola, Agilent Technologies, Capstone, Keithley, Metrowerks, Newark Electronics, National Instruments, and Best Buy.

design—just an optimized combination of current technologies. The paper discusses technical aspects of the topology used to achieve the said objective, the rationale used in choosing this topology, detailed component selection which minimized cost, and the control. Other papers cover issues such as the educational aspect of the UW's involvement [2] and other technical aspects such as project management and heatsink optimization [3].

Finally some conclusions are made and a new total-system-approach design using a high voltage fuel cell is proposed to further reduce the cost of the inverter.

## III. BACKGROUND

The competition objective was to design and build a system, namely an inverter, as shown in Fig. 1, that changed a fuel cell's variable dc output voltage into a standard US domestic 120/240 V<sub>rms</sub> split-phase supply. Table I on the following page shows the inverter's specifications for the Challenge.

The advantage of using a fuel cell to provide the chemical-to-electrical energy conversion is its high fuel-to-electrical-energy efficiency of about 40% including system losses. This can be boosted to as high as 80% by using the heat by-product for home water & space heating or cooling. The particular fuel cell cited for the competition used Proton Exchange Membrane (PEM) cells and had a fuel flow regulation system. This type of fuel cell had two important characteristics:

- (i) the loaded output voltage was nominally 48 V but varied from 42 V to 60 V (open circuit voltage  $\approx$  72 V).
- (ii) the fuel cell had a slow response time which can be modeled by a first order system with  $\tau \approx$  40s.

## IV. DESIGN RATIONALE

The inverter had the following broad requirements: it must provide two 120 V<sub>rms</sub> 60 Hz sinusoidal output voltages, one out of phase with respect the other, from the nominal 48 V fuel cell voltage, while accurately controlling fuel cell current.

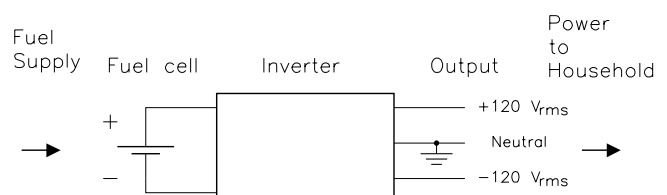


Fig. 1. Overall system block diagram.

TABLE I  
INVERTER SPECIFICATION.

Manufacturing cost	No more than \$500 when scaled to a 10 kW design in high-volume production.
Complete package size	A convenient shape with volume less than 50 L.
Complete package weight	Mass less than 32 kg for a 10 kW unit, not including energy sources or batteries.
Output power capability	10 kW continuous. Single-phase split 120V/240 V, 60 Hz: US domestic.
Input source	48 V dc nominal source (tolerance range 42 V to 72 V) with slow transients.
Overall energy efficiency	Higher than 90% for 10 kW resistive load.
Total harmonic distortion	Output voltage THD: less than 5% when supplying a standard nonlinear load.
Voltage regulation	Output voltage tolerance no wider than $\pm 6\%$ . Frequency $60 \pm 0.1$ Hz.

In this section the possible inverter topologies are discussed and the most cost-effective one is selected. For safety reasons it was decided to provide isolation between the fuel cell and the inverter output, however, this was not a requirement of the competition.

#### A. H-Bridge Driven 60 Hz Transformer—A First Attempt

The first topology considered was the H-bridge driven 60 Hz transformer topology shown in Fig. 2. This has much promise since it is simple and robust, and provides the required voltage boosting and isolation with a minimum of components. However, research showed that this design was not appropriate for the competition since the average 10 kW 60 Hz transformer weighs at least 170 pounds. This exceeds the 70 pound weight limit of the entire inverter. Also these transformers house a significant amount of copper and iron causing prices to be well above \$250.

The conclusion from this was that the inverter must produce the sinusoidal 60 Hz output directly, not through a 60 Hz transformer. The simplest way to do this was to boost the output of the fuel cell to a  $\pm 200$  V split dc bus, use two half-bridge converters, and filter the output. Fig. 3 shows the final topology used for the inverter with a photo of the prototype shown in Fig. 4. The following sections detail the design of each part.

#### B. Boost Stage

##### B.1 Topologies

Initially single and cascade non-isolated boost converters were considered, but providing the large amount of boost was prohibitive due to the large device stresses and parasitic circuit elements. Therefore boost topologies utilizing a high frequency transformer were explored; three are shown in Fig. 5.

MOSFETs were chosen as the switches for all topologies since they are more suitable than IGBTs at this low 48 V

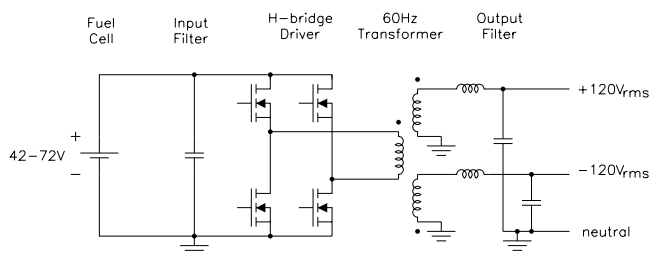


Fig. 2. H-bridge driven 60 Hz transformer topology.

input voltage. Allowing for an overall efficiency of 90% the total input power of 11 kW yields an input current of 230 A. Although all three topologies must process this input current, the current per device differs for the different topologies. The three topologies were quantitatively compared to determine which would be the least expensive. Table II shows the switch current and voltage capability and the switch's  $R_{DS\ ON}$  required for each of the three topologies to stay within the loss budget of 300 W for the boost section.

The comparison shown in Table II reveals that the total switch power—the rms switch current multiplied by the peak switch voltage multiplied by the number of switches—is the same for all topologies: 39 kW. Now MOSFETs can be easily paralleled, so all topologies are equally viable. Clearly topology 5(a) is not a sensible topology due to the simplistic and lossy magnetic core resetting circuit. Topology 5(b) showed promise but using push-pull topologies at high powers ( $> 3$  kW) is problematic and it is prone to staircase-saturation [4]; both these topologies tend to be better suited to lower powers. Topology 5(c) doesn't suffer from the problems mentioned above, scales to high powers, and is robust and well known. For these reasons, it was the topology chosen for the boost section.

##### B.2 Switching Devices

In finding adequate and inexpensive switching devices two discoveries were made:

- (1) the TO-247 (or Super247) packages give the best perfor-

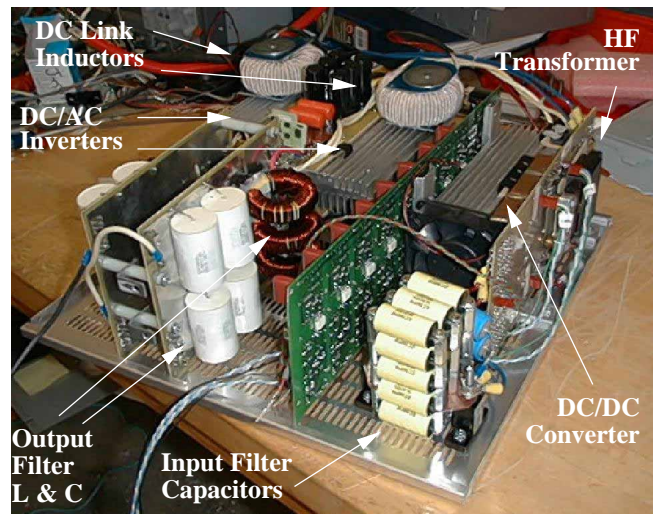


Fig. 4. 10 kW prototype inverter with covers removed.

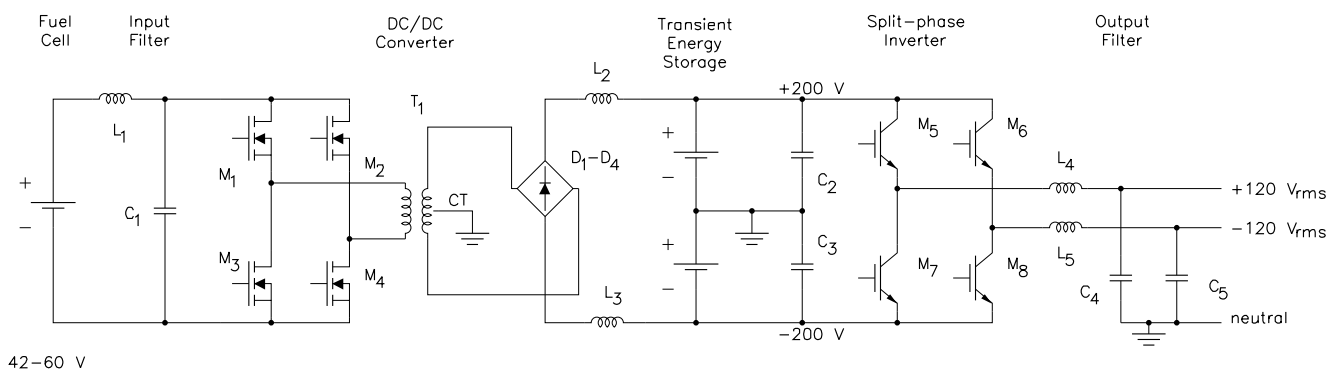
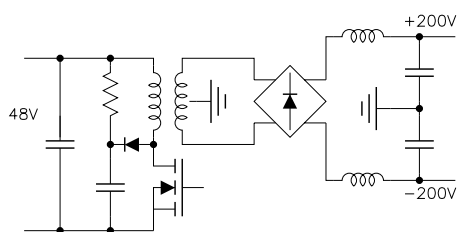


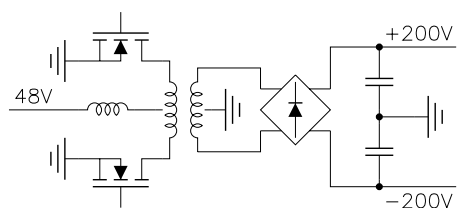
Fig. 3. Schematic of complete inverter.

TABLE II  
COMPARISON OF THE REQUIRED SWITCHES FOR THE THREE CANDIDATE TOPOLOGIES.

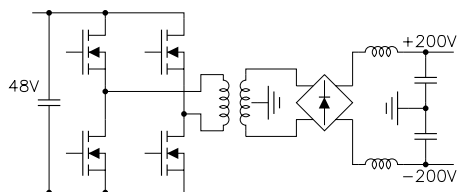
Topology (see Fig. 5)	Number of switches	RMS current	Switch peak voltage	Power of each switch	Required $R_{DS\ ON}$	Total switch power
5(a)	1	325 A <sub>rms</sub>	120 V	39.0 kW	2.84 mΩ	39.0 kW
5(b)	2	162.5 A <sub>rms</sub>	120 V	19.5 kW	5.67 mΩ	39.0 kW
5(c)	4	162.5 A <sub>rms</sub>	60 V	9.75 kW	2.84 mΩ	39.0 kW



(a) single ended forward



(b) current fed push-pull



(c) double ended bridge

Fig. 5. Alternative dc/dc converter topologies.

mance per cost, usually double or triple that of modules (eg. SOT227);

- (2) no single devices met the  $R_{DS\ ON} < 2.85\ m\Omega$  and  $I_D < 162.5\ A_{rms}$  specifications so multiple devices had to be paralleled.

The most promising MOSFET, at a price of only \$5.23<sup>1</sup>, was the IRFP2907 which has an ‘on’ resistance of only 6.75 mΩ hot ( $T_j = 90^\circ C$ ), and a 70 A continuous current limit due to the package. These devices are inexpensive because they are produced in huge quantities for the automotive market. Three of these devices needed to be paralleled per switch to achieve the required ‘on’ resistance (result is 2.25 mΩ) and the current carrying capability (up to 210 A<sub>rms</sub>); therefore 12 devices were required in total. It is noteworthy that many devices would have been required for topology 5(a) and 5(b) also.

Although this may seem like an excessive number of switching devices, it is by far the least expensive configuration. Using the much larger SOT227 packages does not mitigate the need for parallel devices. IR’s highest power 100 V SOT227 device has an ‘on’ resistance 44% higher than the one cited here, and a maximum package current of only 120 A; four of these devices would have to be to achieve the required  $R_{DS\ ON}$ . IXYS’ highest power 100V SOT227 device has an ‘on’ resistance 33% larger and a package thermal current limit of 100 A; again four devices would have to be paralleled.

An attendant plus of this large number of devices is the safety and redundancy of the design: there is plenty of head-room for current spikes. The only concern with using this device is that the peak voltage of the device is 75 V; very close to the open-circuit output voltage of the fuel cell. However this concern is soon calmed when one realizes that power is

<sup>1</sup>Price of devices in quantities of 10,000.

never drawn from the fuel cell when its output voltage is at this value; the fuel cell's auxiliary components have a quiescent power drain and as soon as this power is drawn from the fuel cell, its output voltage drops to a safer level.

### B.3 Input Filter

The particular fuel cell used required the input current to stay within certain bounds; bounds dependent on the fuel flow. Furthermore, the input current ripple must remain within limits or damage could result; the maximum ripple specification is shown in Fig. 6. To keep the current ripple within the required bounds two steps were taken. Firstly, the 120 Hz power ripple was removed by using input current control—see Section IV-E. Secondly, the dc/dc converter switching ripple was filtered using an LC input filter. The selected filter values were 150  $\mu$ F and 6  $\mu$ H. The filter inductor's cost was substantial, due to its 230 A average current rating.

### B.4 High Frequency Transformer

At this point in time a normal ferrite 'E' core transformer is the least expensive HF transformer. However, in large volume mass production a planar transformer built into the structure of the PCB may be cost competitive. The planar transformer used in the 10 kW prototype had one primary turn and 14 secondary turns. A photograph of the transformer is shown in Fig. 7. The TO-247 MOSFET shows how small the transformer is. The transformer had a calculated loss of 40 W at full load and cost \$40<sup>1</sup>.

### B.5 Rectifier Devices

Although a half-wave rectifier could have been used after the transformer, it was less expensive to use a full-wave rectifier because it allowed the use of lower voltage diodes and a lower voltage transformer secondary (having fewer turns). The rectifier devices chosen were fast recovery 1200 V, 52 A epitaxial TO-247 diodes: IXYS DSEI60-12A with a price of \$3.83<sup>2</sup>.

### B.6 Intermediate DC-Link and Transient Energy Storage

Since the fuel cell responds slowly the load power would not match by the power output from the fuel cell during transients; there would be a power deficiency or excess. The fuel cell could be damaged if more current is taken than it can supply, so current demand should never exceed available

<sup>2</sup>Price of devices in quantities of 1,000.

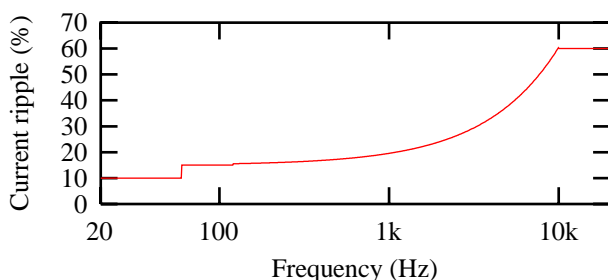


Fig. 6. Fuel cell maximum input current ripple specification.

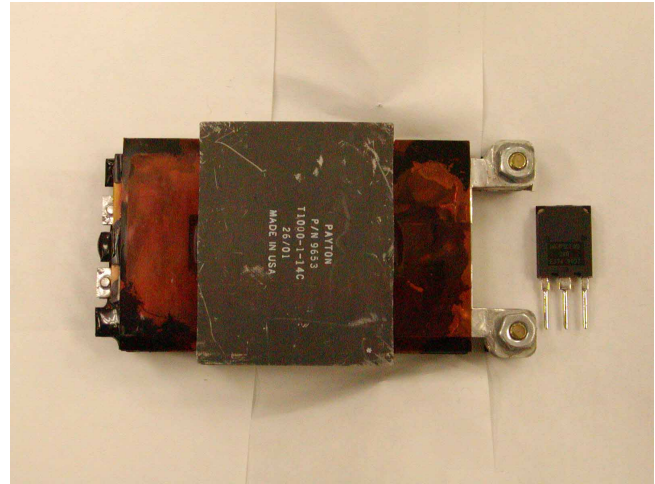


Fig. 7. A photograph of the 10 kW planar transformer used in the prototype. It had one primary turn and 14 secondary turns. The TO-247 MOSFET shows its small size.

current. Current demand may be less than available current, but this results in unused fuel being exhausted from the fuel cell. For these two reasons some energy storage was required to sink/source the power difference. Lead acid batteries were the required form of energy storage for the competition.

It was up to the designer to decide where to place these batteries in the system and what voltage to use. Initially it was thought that low voltage batteries would be best, but then a bi-directional dc/dc converter would be required to charge/discharge them. Not only is this very costly, but the power delivered from the fuel cell to the batteries is processed twice and it is processed twice again going from the batteries to the load. This quadruple processing of power, which occurs whenever there is a power transient, is inefficient. Furthermore, both the boost circuit, and the battery dc/dc converter must be rated at the full 10 kW so the cost would be prohibitive.

A better system, and the one that was implemented, had the batteries directly connected to the split dc bus. This required no extra components, and all power was only processed twice. The rules limit the capacity of the lead-acid batteries to 3.3 kWh for the 10 kW design. To obtain  $\pm$ 200V thirty-two 12 V batteries were connected in series. This limited the capacity of each battery to approximately 8 Ah; the design used Powersonic's PS-1282L 12 V, 8 Ah batteries (ESR of 20 m $\Omega$ ). The two 100  $\mu$ H, 25 A inductors between the rectifier and the batteries completed the boost design. As can be seen in Fig. 4 these two inductors were large and their cost was substantial.

## C. Inverter Output Stage

### C.1 Topology

To create the split-phase 120 V 60 Hz output from the  $\pm$ 200 V dc bus two half-bridge converters were used; one is shown in Fig. 8. Although unipolar switching is desirable bipolar voltage switching was required to achieve the split-phase output with the minimum number of switches. Power was supplied from the split dc bus with the grounded center point supplying neutral current.

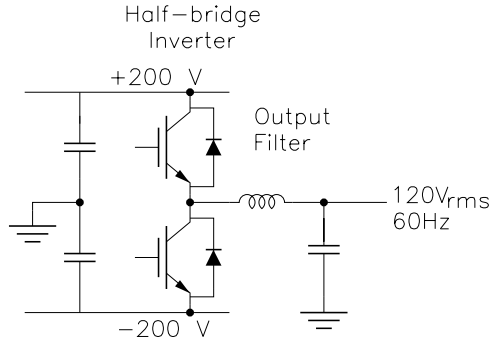


Fig. 8. Half-bridge with filter.

### C.2 Devices

Using maximum load values of 10 kW, 240 V<sub>rms</sub> and 0.8 pf, the devices required a current capability of 57 A<sub>rms</sub> and a 400 V voltage blocking capability. IGBTs are better than MOSFETs at these voltage levels. 600 V 85 A IRG4PSC71KD IGBTs with integrated ultrafast soft-recovery diodes were chosen based on their current and voltage ratings, device losses and, most importantly, the cost. These devices had a Super247 package,  $V_{CE\,Sat} = 1.83\text{ V}$  and a diode forward voltage drop of 1.4 V.

Increasing the switching frequency decreases the required size of the output filter, reducing cost, but this also increases losses in the inverter. 20 kHz was the highest switching frequency possible while keeping within the 500 W inverter loss budget, and was therefore used. Using this switching frequency the switching and conduction losses were calculated for each switch and its associated anti-parallel diode for a 10 kW inductive load. Using these results the total loss per device package was calculated, as was the loss for the two inverters. The results are tabulated in Table III. Low-cost RC turn-off snubbers were used to reduce  $dv/dt$  and EMI. Snubber loss was calculated to be 30 W per inverter.

### C.3 Output Filter

The output filter needed to be designed to be large enough to passively filter the PWM voltage ripple and small enough to allow the controller to control the output voltage using the control shown in Section IV-E, while being optimized for minimum cost. Final filter component values were 100  $\mu\text{H}$  and 80  $\mu\text{F}$ .

The peak output current was calculated to be 80 A. To keep the cost low powdered iron toroidal inductors were used with an estimated cost of \$55 each.

The output filter capacitors were the polypropylene type because they could sustain the large continuous high frequency current. To obtain the required capacitance a number of capacitors had to be paralleled resulting in a larger than necessary current rating and hence an overdesign, however

TABLE III

INVERTER LOSS BREAKDOWN FOR 10 kW 0.8 PF INDUCTIVE LOAD WITH A SWITCHING FREQUENCY OF 20kHz.

Transistor		Diode		Device Losses	
Sw.	Cond.	Sw.	Cond.	Package	Inverters
50.46	34.25	0	26.22	110.94	443.77

these capacitors are relatively inexpensive.

### C.4 DC Bus Capacitors

To extend battery life, battery current should not contain large ripple or  $di/dt$ , therefore, capacitors were placed across each battery string. The capacitors chosen were Cornell Dubilier type 330, 560  $\mu\text{F}$  capacitors with an ESR of 85 m $\Omega$ . In this case six capacitors had to be paralleled across each bus to sustain the switching frequency ripple current, resulting in a larger than necessary capacitance and hence an overdesign. Unfortunately this overdesign came at a higher cost than the filter capacitor overdesign. With these capacitors the switching frequency battery current was only 1.2 A<sub>rms</sub>.

The 120 Hz battery current was substantial with the proposed design. To stop this a bus inductor would have to be used, and the bus capacitance made much larger. However, this is very costly. The batteries used could withstand the 120Hz ripple.

### D. Heatsink

The heatsink is a vital component of the inverter, and represents a significant cost. Much work was done on the heatsink design [3]. The least expensive design used six extruded aluminum heatsink elements and three computer fans in the arrangement shown in Fig. 9.

### E. Control

The following sections describe the control algorithms used and implementation details. The control designs for the dc/dc converter and the inverters are given in the first two sections. The third section describes controller hardware.

#### E.1 DC/DC Converter Control

The control requirements for the dc/dc converter are very different from a conventional application. Here, the fuel cell source has control signals of its own and is an integral part of the controller. In addition, a fuel cell has many restrictions on how energy is drawn from it. Switching frequency current must be passively filtered and the dc/dc controller must not allow low frequency ( $\leq 120\text{ Hz}$ ) current to be drawn from the fuel cell. See Fig. 6 for the current-ripple specification.

The fuel cell used had a “power request” input and a “power available” output, with a first order response ( $\tau \approx 40\text{ s}$ ). This response time was due to the mechanical nature of the fuel cell’s fuel-flow regulator. Drawing too much power damages the fuel cell and drawing too little wastes fuel: the converter should draw power equal to the “power available” signal.

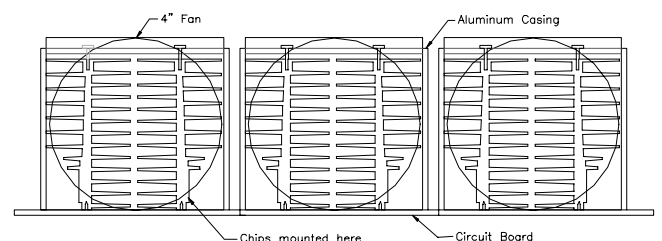


Fig. 9. Final heatsink design using six extruded aluminum elements and three 4-inch computer fans.

The dc/dc controller had two separate sections: one determines how much power to be requested from the fuel cell (the power request controller), and the other controls the power drawn from the fuel cell (the power tracking controller). Fig. 10 shows the control block diagram. Note that labeled states are average, low-pass-filtered values.

The power request controller is simply a proportional-integral (PI) controller for bus voltage. It generates an output current command,  $I_o^*$ , then multiplies  $I_o^*$  by the bus voltage to yield  $P^*$ , the requested power. This provides a bus-voltage-independent gain.

The power tracking controller must accurately control average current drawn from the fuel cell. Ramp-compensated, peak-switch-current turn-off, clocked turn-on Peak Current Mode Control (PCMC) [5] is the most common current controller used in industry and was selected. PCMC provides the necessary degree of input current control and prevents overcurrent due to transformer saturation. It also eliminates the possibility of transformer “staircase saturation” due to the cumulative effect of slight gate-pulse-duration imbalance [4]. A single Hall-effect type current sensor placed between the input filter and the MOSFETs was used for PCMC current feedback.

PCMC naturally controls peak current, not average current. Average current control may be obtained with PCMC by closing an average (filtered) current feedback PI loop around the PCMC block [6]. Note that the PCMC block in Fig. 10 includes the high frequency current feedback loop used to detect peak current. In addition to feedback, a function block “Fn” is included to map the desired average current to the peak-current-command input to the PCMC block. The true relationship between the peak current and average current is a nonlinear function of input and output voltage, output filter inductance and switching frequency. Non-ideal component characteristics such as stray inductance and saturation also have an effect on this relationship. However, a simple constant value approximation can be used, because the feedback loop can correct for the error. A value of two was a good initial approximation corresponding to the boundary between continuous and discontinuous current. Improved performance can be obtained by using a lookup table, especially when the inductor current is discontinuous.

Since the inverter load current is changing at twice the line frequency, a significant current fluctuation is present in the bus capacitors and batteries. Parasitic impedance in the capacitors/batteries can therefore cause a voltage ripple on the bus. To ensure that this varying bus voltage does not cause pulsating power to flow from the fuel cell, the bandwidth of the voltage feedback used for the fuel cell power request must be less than the bus voltage ripple frequency. Also, the bandwidth of the power tracking controller must be greater than that of the bus voltage ripple. Therefore, the low-pass filter corner frequencies chosen were 10 Hz and 1 kHz respectively.

The power tracking controller has a constant-power-drawing nature created by the combination of the divide-by-voltage function and PCMC. Thus, the seemingly benign input LC filter can be a source of instability [5]. The strong input filter resonance must be damped to prevent this insta-

bility. Simulations showed that an RC damper, placed in parallel with the filter capacitor, with a damping capacitor having two-thirds of the capacitance of the filter capacitor and a resistor tuned to give maximum damping ( $C_{damp} = 100 \mu\text{F}, R_{damp} = 0.3 \Omega$ ) provided enough damping for the system to be stable. The steady state rms current in the damper was low, consisting of only a small switching frequency ripple. Consequently, there was less than 10 W of steady-state loss in the resistor. Placing a resistor in parallel with the inductor is also a viable solution [5], but the losses would have been higher in this case. The division function and PCMC combination in the power tracking controller attempts to maintain constant power flow. Using the fuel cell voltage for the voltage input signal  $V_I$ , rather than the input capacitor voltage greatly reduced the effect that the division function had on input filter resonance. Stability was further improved by low-pass filtering the input voltage signal at 1 kHz, because this frequency is below the 5 kHz input filter resonance frequency.

## E.2 Inverter Control

An observer-based single-phase-inverter controller for a UPS application was proposed in [7]. This approach gives very good performance and requires no current sensors. A simplified form of this approach was used for control of each of the two inverter phase legs, with the resultant diagram shown in Fig. 11. The command feedforward section of the controller was eliminated for simplicity. The line-frequency voltage drop across the output inductor is small and the feedback controller can easily correct for this error. Also, bus voltage decoupling was further developed to include decoupling of voltage imbalance between the top and bottom halves of the bus. The voltages of the two halves was close because the center tap of the transformer was connected to the neutral point of the bus: more current flows to the half that has lower voltage. However, some imbalance may remain due to nonidentical battery cells. The inverter modulation (without feedback) is given in (1).

$$M = \frac{1}{2} - \frac{V_{Bus+} - V_{Bus-}}{2(V_{Bus+} + V_{Bus-})} + \frac{120\sqrt{2}\sin(2\pi \times 60t)}{V_{Bus+} + V_{Bus-}} \quad (1)$$

Handling nonlinear loads was the most challenging inverter control issue. Loads such as diode-bridge rectifiers used in computers and most other household electronics draw large current spikes that excite a resonance in the inverter output filter. Matlab/Simulink simulation results shown in Fig. 12 show the performance of the inverter with open and closed loop control. The load used for this simulation was a

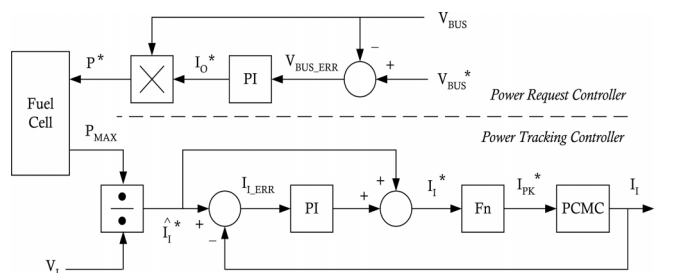


Fig. 10. DC/DC converter control block diagram.

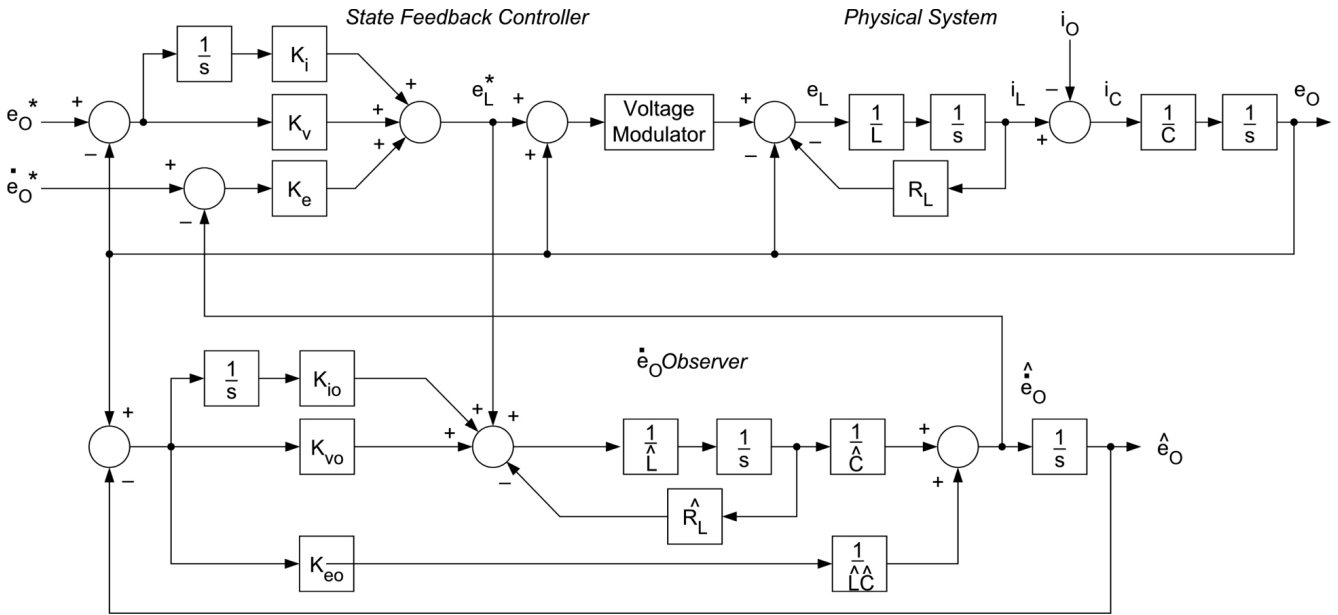


Fig. 11. Simplified observer based single phase inverter controller.

3 kW diode bridge rectifier, equivalent to 20 computer power supplies (CPS) in parallel. While this is an unrealistically difficult load, the voltage THD was still under the required value of 5% given in the specifications shown in Table I.

### E.3 Control Hardware

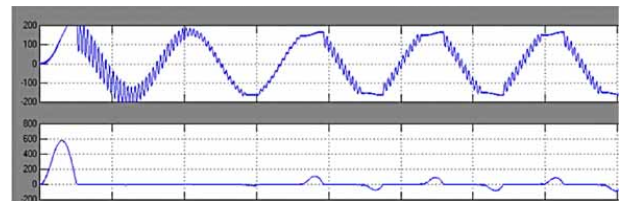
The heart of the control system was the DSP chip. The DSP must be able to handle all of the previously mentioned tasks simultaneously, which required a large amount of processing speed as well as enough I/O channel connections. Flash memory can save a significant amount of development time and is also an advantage for a final product; the firmware may be upgraded easily in the field. This may need to be done when the batteries are replaced, as battery technology is always changing.

A simple 8-bit PIC microcontroller was first considered, however several shortcomings were soon apparent. A series of Motorola 16-bit DSP chips were found to have better performance and greater flexibility, yet only costs approximately \$5.50 each in large quantities. The DSP56F807 was chosen. It operates at 40 MIPS, has flash memory, a serial bus and many other I/O channels. It features two banks of six PWM outputs with programmable dead-time, which allows the one chip to control both the dc/dc converter and the inverters, with the exception of the PCMC, which required additional comparator, logic and ramp generation circuitry.

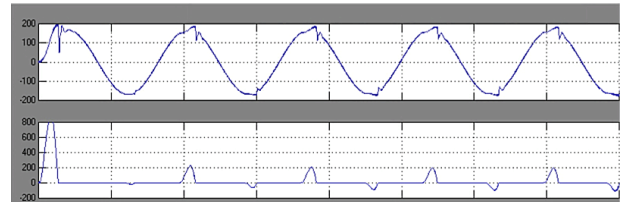
TABLE IV

SIMULATED OUTPUT VOLTAGE DISTORTION IN % THD FOR VARIOUS LOADS.

Control	Linear load	3 CPSs	20 CPSs
Open Loop	1%	6.2%	14%
Closed loop	1%	1.9%	4.8%



(a) Open loop



(b) Closed loop

Fig. 12. Inverter simulation results with 20 CPS loads. top: voltage (V); bottom: current (A); horizontal: time (10ms/div.).

## V. EDUCATIONAL EXPERIENCE

### A. Team Structure and Project Management/Organization

The University of Wisconsin's team was composed of 22 student members and two faculty advisers. Of the 22 students, 15 earned credit toward their degrees and 11 were undergraduates.

Since the inverter comprised five main sections, the team was divided into five groups: (1) the fuel cell to dc-link boost group, (2) the dc-link and battery group, (3) the H-bridge split-phase inverter group, (4) the control group, and (5) the heatsink group. The students divided among the groups, sometimes participating in multiple groups; five group leaders and one chairperson completed the team. The UW FEC

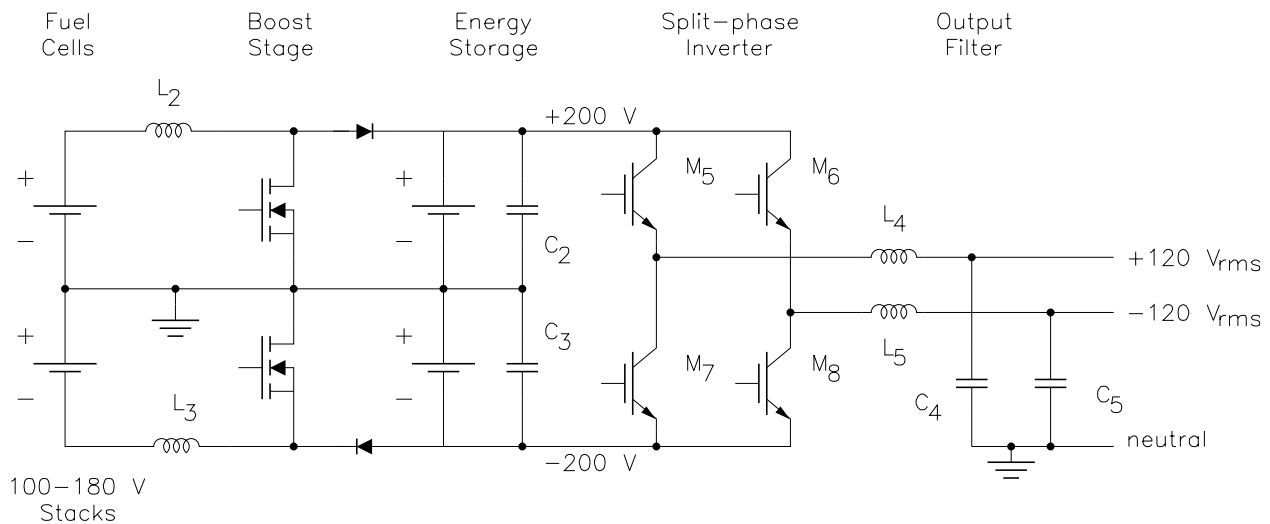


Fig. 13. Future high voltage fuel cell inverter.

Team was selected to be among the top five teams and competed in the final competition held in Morgantown, WV in August 2001. More information on the structure and management of the team can be found in [2].

## VI. CONCLUSIONS

In the Fall of 2000 the US Department of Energy and the IEEE setup and sponsored a national US student competition to develop a very-low-cost fuel cell powered dc/ac inverter to aid the development of fuel cell distributed power. The University of Wisconsin—Madison & Platteville campuses had a multidisciplinary team of 22 graduate and undergraduate students participate in the competition. By examining various topologies the team was able to select the most cost effective topology. A 10 kW prototype was built according to the design and tested at the FEC final competition.

This paper discussed the topology used to achieve the said objective, the rationale used in choosing this topology, detailed component selection optimized to minimize cost, and the dc/dc and dc/ac control.

## VII. FUTURE WORK

For the competition the fuel cell's nominal output voltage was 48 V and, therefore, a boost stage was required. It is interesting to note that this boost stage incurs a large percentage of the cost of this inverter and a substantial percentage of

the loss. There was an inherent mismatch between the competition's fuel cell output characteristic and the requirements of ac domestic power; an issue also present in other renewable energy sources such as photovoltaic cells.

In light of this a new topology which uses two nominal 120 V fuel cells is proposed, and shown in Fig. 13. This design has the boost stage built into the input filter and needs no transformer or intermediate dc-link inductors. With the input voltage being higher, the size of the input inductors becomes smaller; it is estimated that this design would reduce the cost by about 30%.

## REFERENCES

- [1] US Department of Energy, "http://www.energychallenge.org," Jan. 2001.
- [2] J. J. Nelson and A. M. Tuckey, "Education is the future of alternative energy research," in *EPE-PEMC 2002 Conference*, Sep. 2002, in press.
- [3] J. J. Nelson and A. M. Tuckey, "A low cost 10 kw fuel cell inverter for domestic power," in *EPE-PEMC 2002 Conference*, Sep. 2002, in press.
- [4] K. Billings, *Switchmode Power Supply Handbook*, New York: McGraw-Hill, 1989.
- [5] A. S. Kislovski, R. Redl, and N. O. Sokal, *Dynamic Analysis of Switching-Mode DC/DC Converters*, New York: Van Nostrand Reinhold, 1991.
- [6] J. Kruse, "DC-link capacitor size minimization in nonregenerating voltage source inverter motor drives," M.S. thesis, University of Wisconsin—Madison, 2002, in press.
- [7] M. J. Ryan, W. E. Brumsickle, and R. D. Lorenz, "Control topology options for single-phase UPS inverters," *IEEE Trans. Ind. Appl.*, vol. 33, no. 2, pp. 493–501, Mar./Apr. 1997.